

Benzyl and Cumyl Dithiocarbamates as Chain Transfer Agents in the RAFT Polymerization of *N*-Isopropylacrylamide. In Situ FT-NIR and MALDI–TOF MS Investigation

Christine Schilli, Michael G. Lanzendörfer, and Axel H. E. Müller*

Makromolekulare Chemie II, Universität Bayreuth, 95440 Bayreuth, Germany

Received December 4, 2001; Revised Manuscript Received May 28, 2002

ABSTRACT: The principles of RAFT polymerization were applied to the polymerization of *N*-isopropylacrylamide (NIPAAm), which was carried out in the presence of the dithiocarbamates benzyl 1-pyrrolinecarbodithioate and cumyl 1-pyrrolinecarbodithioate, respectively, as chain transfer agents in 1,4-dioxane at 60 °C. A kinetic investigation using in situ FT-NIR spectroscopy shows very long induction periods which depend on the nature and concentration of the chain transfer agent. The resulting polymers have polydispersity indices $M_w/M_n < 1.3$ and have been investigated by MALDI–TOF mass spectrometry, GPC, NMR, and UV spectroscopy. The expected end group signals for chain transfer agent (CTA) and initiator could be identified together with fragmentation of the dithioester end group under MALDI conditions. The number-average molecular weights obtained by MALDI–TOF MS are significantly lower than those obtained by GPC with polystyrene calibration. With the use of the abovementioned dithiocarbamates, new thiocarbonylthio compounds have been applied in the RAFT polymerization of *N*-isopropylacrylamide.

Introduction

Recently, the synthesis of polymers via reversible addition–fragmentation chain transfer (RAFT) polymerization has gained importance due to its great versatility, its compatibility with a wide range of monomers, the control of the molecular weights, and the low polydispersities of the resultant polymers. It also offers all advantages of a conventional free radical polymerization; e.g., the same range of temperatures, monomers, initiators, and solvents can be applied.^{1–3} The polymerization is carried out in the presence of thiocarbonylthio compounds of general structure $Z-C(=S)S-R$ that act as reversible addition–fragmentation chain transfer agents and results in the formation of end-functionalized polymers.⁴

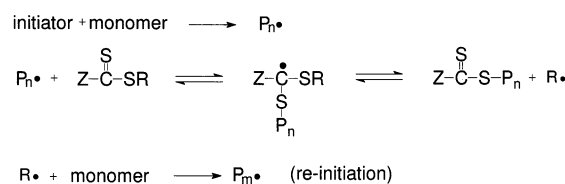
The process is performed by adding a suitable chain transfer agent (thiocarbonylthio compound) to an otherwise conventional free radical polymerization mixture, and it provides living polymers of predetermined molecular weight and of narrow polydispersity (usually $M_w/M_n < 1.2$).

The mechanism of the RAFT process is believed to involve a series of reversible addition–fragmentation steps (Scheme 1). Addition of a propagating radical P_n^* to the thiocarbonylthio compound gives an adduct radical which fragments to a polymeric thiocarbonylthio compound and a new radical R^* . The radical R^* then reinitiates polymerization to give a new propagating radical P_m^* . Subsequent addition–fragmentation steps set up an equilibrium between the propagating radicals P_n^* and P_m^* and the dormant polymeric thiocarbonylthio compounds by way of an intermediate radical. Equilibration of the growing chains gives rise to a narrow molecular weight distribution.^{2,3,5}

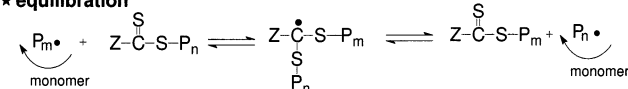
The selection of the transfer agent is crucial for the synthesis of low-polydispersity products. It does not only depend on the chain transfer constant but also on the

Scheme 1. Mechanism of the RAFT Process

★ addition-fragmentation



★ equilibration



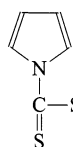
structure of the transfer agent. The R moiety should be a good homolytic leaving group, and the formed R^* radical should be able to reinitiate the polymerization. The Z group regulates the reactivity toward radical addition. The Z moiety usually includes alkyl, aryl, or heterocyclic groups, while the R group is either of alkyl or aryl nature.⁴

At present, reliable kinetic investigations of the RAFT polymerizations are still rare.^{6,7} One method of investigating the kinetics in situ is FT-NIR spectroscopy. It provides detailed information on the course of the polymerization.⁸ It will also reveal any peculiarities of the polymerization reaction, such as an induction period.

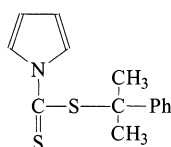
Beside the interesting properties of its polymer, *N*-isopropylacrylamide (NIPAAm) is an ideal monomer for FT-NIR measurements as it shows a distinct overtone of the vinylic CH stretching at 6157 cm^{-1} . Variation of this band is followed throughout the reaction until it disappears at complete monomer conversion. Besides the advantages of investigating the kinetics of the reaction on-line, FT-NIR also provides reliable conversion data as oligomeric fractions may not be taken into account with a gravimetric determination of the conversion. To our knowledge, this is the first determination of RAFT kinetics by in situ FT-NIR spectroscopy. NIR

* Corresponding author. Fax: +49-921-553393. E-mail: axel.mueller@uni-bayreuth.de.

Scheme 2. Structures of the Chain Transfer Agents



Benzyl 1-pyrrolicarbodithioate (1)



Cumyl 1-pyrrolicarbodithioate (2)

offers several advantages as compared to mid-IR spectroscopy. The latter requires ATR equipment in conjunction with expensive conduits or fiber-optic cables.

NIPAAm has been polymerized successfully via RAFT by Ganachaud et al. using benzyl and cumyl dithiobenzoate as chain transfer agents.⁹ Our experiments were carried out using two different chain transfer agents, namely benzyl 1-pyrrolicarbodithioate (benzyl CTA, **1**) and cumyl 1-pyrrolicarbodithioate (cumyl CTA, **2**) (Scheme 2). Cumyl 1-pyrrolicarbodithioate is a RAFT agent that has been first synthesized in our group.

The synthesized polymers have polydispersities $M_w/M_n < 1.3$. With the use of the abovementioned dithiocarbamates, new thiocarbonylthio compounds have been applied in the RAFT polymerization of NIPAAm. The resulting polymers were investigated and structurally characterized by MALDI-TOF mass spectroscopy for absolute mass determination and end group analysis.

Experimental Section

Materials. *N*-Isopropylacrylamide (Aldrich, 97%) was recrystallized twice from benzene/hexane 3:2 (v:v) and dried under vacuum prior to use. 1,4-Dioxane (Merck, p.a.) was refluxed over potassium for 3 d and then distilled. Azobisisobutyronitrile (AIBN, Fluka, purum) was recrystallized from methanol and dried under vacuum prior to use. DMSO (puriss., over molecular sieves) was purchased from Fluka and used as received. Pyrrole (Fluka, purum) was distilled over NaOH prior to use. CS₂ (purum) and benzyl chloride (purum) were purchased from Fluka and used as received. NaH was used in the form of a free-flowing powder, moistened with oil (55–65%, Fluka).

Synthesis of Benzyl 1-Pyrrolicarbodithioate (1). The synthesis of this chain transfer agent was carried out according to the procedure reported in the literature.¹⁰

Synthesis of Cumyl 1-Pyrrolicarbodithioate (2). A suspension of NaH (0.48 g, 20 mmol) in DMSO (20 mL) was prepared. Freshly distilled pyrrole (1.34 g, 20 mmol) was added under vigorous stirring. The yellow solution was then stirred for another 30 min at room temperature. The solution was cooled to 20 °C, and CS₂ (1.52 g, 20 mmol) was added dropwise. The resultant reddish orange solution was stirred for 30 min at room temperature, and then cumyl bromide (3.98 g, 20 mmol) was added. After the mixture was stirred for 2 h, water (20 mL) and then diethyl ether (20 mL) were added. The organic layer was separated, and the aqueous layer was extracted three times with diethyl ether (40 mL). The combined extracts were dried over MgSO₄ and filtered, and the solvent was evaporated. The crude product was subjected to column chromatography (silicagel 60, mesh 70–230) with cyclohexane/ethyl acetate 95:5 (v:v) as eluent. The main fraction was bright orange. The solvent was evaporated and the product dried under vacuum to yield an orange oil. Yield: 48%. ¹H NMR (CDCl₃): δ 1.95 (s, 6H, CH₃), 6.20 (dd, 2H, pyrrole CH), 7.15–7.28 (m, 5H, phenylic CH), 7.56 (dd, 2H, pyrrole CH).

RAFT Polymerization. For the polymerization series conducted at different benzyl CTA (**1**) concentrations, stock solutions were prepared with a monomer concentration of 1.742 mol/L, an initiator concentration of 6.90 mmol/L and CTA concentrations of 3.92×10^{-2} , 1.96×10^{-2} , 9.80×10^{-3} , and 4.90×10^{-3} mol/L. Chain transfer agents **1** (0.915–0.114

g; $3.92\text{--}0.49$ mmol) and **2** (0.512 g, 1.96 mmol), respectively, were dissolved in 1,4-dioxane (98 mL), and the solutions were degassed by three freeze–thaw evacuation cycles. AIBN (0.115 g, 0.70 mmol) was dissolved in 1,4-dioxane (2 mL) and degassed by three freeze–thaw evacuation cycles. The monomer (20.37 g, 0.18 mol) was added via a Schlenk tube under nitrogen to the solution of the chain transfer agent in dioxane. After complete dissolution of the monomer and heating of the mixture to 60 °C (temperature of oil bath), the initiator solution was injected with a syringe. All polymerizations were conducted under nitrogen atmosphere and samples were withdrawn at different time intervals. The samples were immediately immersed into liquid nitrogen and subsequently freeze-dried. The residues were dried under vacuum, whereby residual monomer was removed by sublimation. The dried substances were dissolved in THF + 0.25% tetrabutylammoniumbromide for GPC analysis.

Hydrolysis of the Dithiocarbamate End Groups in Poly(NIPAAm). The dithio end groups of the obtained polymer samples were hydrolyzed to yield the corresponding thiol-terminated polymers under basic conditions. For this purpose, the polymer was dissolved in a mixture of MeOH/aq. 28% NaOH (2:1) and stirred under nitrogen overnight. The reaction mixture was acidified with 88% formic acid, MeOH was evaporated and the residue was freeze-dried. The solid obtained was directly subjected to MALDI-TOF analysis.

Kinetic Measurements. Fourier transform near-infrared (FT-NIR) spectroscopy was performed using a Nicolet Magna 560 FT-NIR instrument with a PbS detector and a fiber-optic deep-temperature immersion probe (Hellma, quartz glass Suprasil 300, path length 10 mm). Data processing was performed with Nicolet's OMNIC Series software. Each spectrum was constructed from 32 scans with a resolution of 4 cm⁻¹. The total collection time per spectrum was approximately 22 s. Prior to the measurements, a blank spectrum was recorded with the solution of the corresponding chain transfer agent in 1,4-dioxane at 60 °C. After addition of the monomer, the measurement was started and the initiator solution was injected shortly after. The baseline for signal height determination was drawn from 7000 to 5035 cm⁻¹. ¹H NMR spectra were recorded on a Bruker 300 MHz instrument using TMS as internal standard. UV measurements were performed on a Lambda15 UV-vis spectrophotometer (Perkin-Elmer) in the wavelength range from 190 to 550 nm.

Polymer Characterization. Gel permeation chromatography (GPC) was performed on a Waters Associates liquid chromatograph equipped with an RI detector and a UV detector (λ = 254 nm) at a temperature of 25 °C. PSS SDVgel columns (30 × 8 mm, 5 μm particle size) with 10², 10³, 10⁴, and 10⁵ Å pore sizes were used. THF + 0.25 wt % of tetrabutylammonium bromide was used as an eluent (flow rate 0.5 mL/min). The injection volume was 100 μL and a Spectra Physics P 100 pump was used. As an internal standard, *o*-dichlorobenzene was used. Polystyrene standards were used for calibration.

MALDI-TOF mass spectrometry was performed on a Bruker Reflex III equipped with a 337 nm N₂ laser in the reflector mode and 20 kV acceleration voltage. Dithranol (Aldrich, 97%) was used as matrix. Sodium or potassium trifluoroacetate was added for ion formation. Samples were prepared from THF solution by mixing matrix (20 mg/mL), sample (10 mg/mL) and salt (10 mg/mL) in a ratio of 10:1:1. The number-average molecular weights, M_n , of the polymer samples were determined in the linear mode.

Results and Discussion

Polymerization Kinetics. The course of the polymerization was followed by in situ FT-NIR spectroscopy. In addition, samples were withdrawn at different time intervals in order to determine the molecular weights and the development of the molecular weight distribution with conversion. FT-NIR allows the continuous determination of monomer conversion in controlled

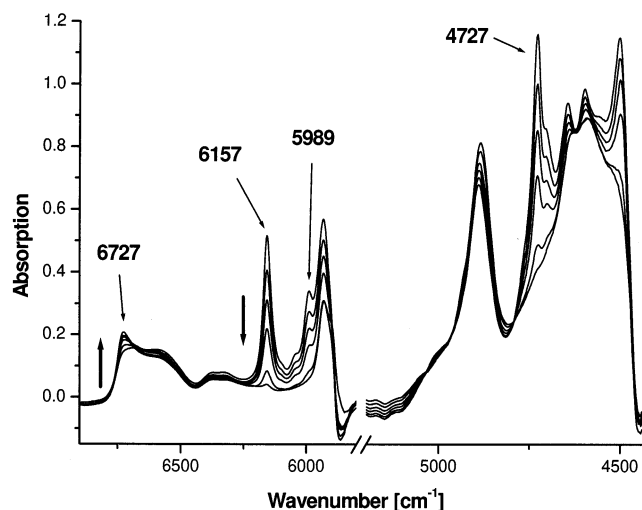


Figure 1. Evolution of various vibration overtone bands (after 2, 255, 283, 323, 551, and 1519 min, respectively) in the RAFT polymerization of NIPAAm in dioxane using benzyl 1-pyrrole-carbodithioate as chain transfer agent.

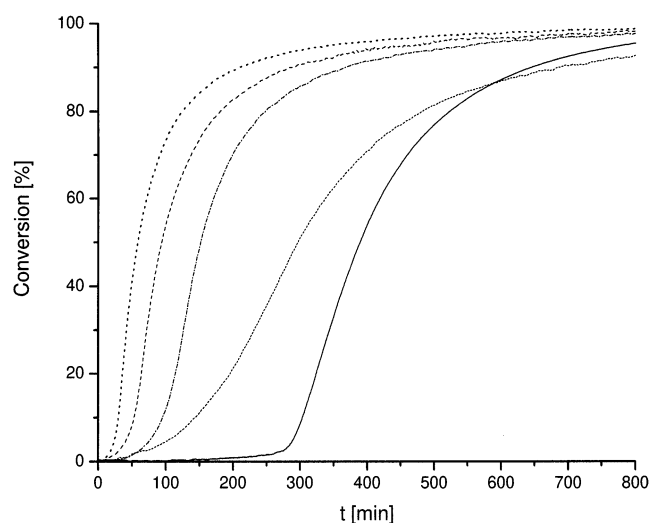


Figure 2. Time-conversion plot during the initial 800 min for the RAFT polymerization of NIPAAm in dioxane at 60 °C with (···) benzyl CTA with $[CTA]_0 = 3.92 \times 10^{-2}$, (---) 1.96×10^{-2} , (—) 9.80×10^{-3} , and (●●) 4.90×10^{-3} mol/L and (—) cumyl CTA with $[CTA]_0 = 1.96 \times 10^{-2}$ mol/L.

radical polymerization.^{11,12} The determination of the monomer conversion can be more reliable with FT-NIR spectroscopy than with gravimetry. With a gravimetric determination of the conversion by precipitation, soluble oligomeric fractions will not be taken into account. Even GC determination of the residual monomer was not reliable as the conversions determined for the same sample varied considerably due to sublimation of the monomer and evaporation of the internal standard (*n*-decane).

In the FT-NIR measurements, spectra of the reaction mixture were recorded every 30 s. The spectra cover the range from 4500 to 7500 cm^{-1} . The variation of the intensity of the bands with time was followed. For the evaluation of the FT-NIR results, monomer bands were chosen that do not considerably overlap other bands, e.g., of the solvent or polymer.

For *N*-isopropylacrylamide, the vinylic stretching overtone was found at 6157 cm^{-1} and used to determine conversion. Other signals (5989 cm^{-1} and approximately 5930 cm^{-1}) were too close to the solvent cutoff and thus

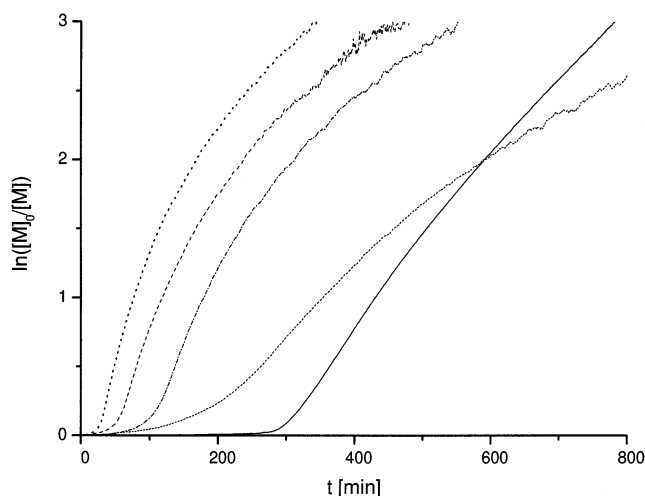


Figure 3. First-order time-conversion plots for the RAFT polymerizations with benzyl and cumyl CTA, symbols see Figure 2.

Table 1. Induction Times, t_{ind} , Apparent Rate Constants, k_{app} , Number-Average Molecular Weights, and Polydispersity Indices at Full Monomer Conversion for the RAFT Polymerizations of NIPAAm^a

CTA	$[CTA]_0$ (mmol/L)	t_{ind} (min)	$10^4 k_{\text{app}}$ (s^{-1})	$M_{n,\text{theor}}$	$M_{n,\text{exp}}^b$	M_w/M_n^c
benzyl	39.2	133	0.81	5300	3900	1.28
	19.6	88	1.9	10 300	6400	1.37
	9.8	44	2.2	20 300	16 800	1.25
	4.9	23	3.4	40 400	38 800	1.21
cumyl	19.6	280	1.2	10 300	15 200	1.09 ^b

^a At 60 °C in dioxane. $[NIPAAm]_0 = 1.742$ mol/L, and $[AIBN]_0 = 6.90$ mmol/L. ^b Determined by MALDI-TOF MS. ^c Determined by GPC using calibration with poly(NIPAAm) samples.

were not used. In the range of combination vibrations, additional peaks were determined and assigned as monomer signals (4727, 4644, 4597, 4500 cm^{-1}). An absorption at 6727 cm^{-1} increasing during the polymerization was attributed to the formation of poly(*N*-isopropylacrylamide). The signal intensities were converted into conversions by evaluating the intensities for zero monomer conversion and for total conversion. Figure 1 shows the evolution of the FT-NIR bands with time for the RAFT polymerization of NIPAAm.

The time-conversion plots obtained from FT-NIR spectroscopy show long induction periods for both polymerization processes (Figures 2 and 3). After the induction period, the first-order time-conversion plots (Figure 3) show slowly decreasing slopes indicating a slow decrease of the active radical concentration.

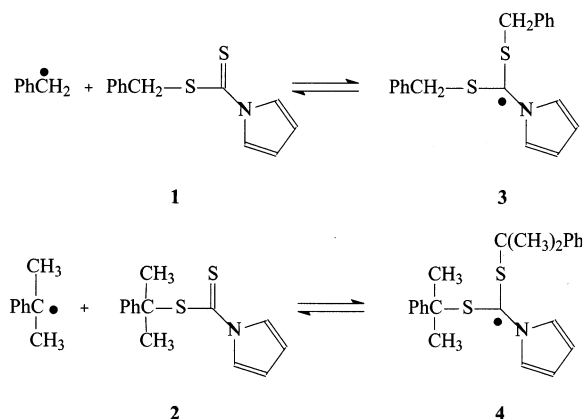
For the quantitative determination of the induction periods, a tangent was fitted to the steep part of the curves. The values of the induction periods were obtained from the point of intersection of this tangent with the time axis. The induction periods amount to ca. 280 min for the NIPAAm/cumyl CTA system and to ca. 88 min for the NIPAAm/benzyl CTA system at a CTA concentration of 1.96×10^{-2} mol/L.

A polymerization series conducted at different benzyl CTA concentrations shows that the observed induction periods increase with increasing CTA concentration. Furthermore, the apparent rate constants, k_{app} , for the polymerization were determined as the slopes of the first-order time-conversion plots at the inflection point (Table 1). The increasing induction periods are accompanied by a decrease of the apparent rate constants,

Table 2. Masses of Expected Reaction Products

	structure	<i>X</i>		monoisotopic mass
(i) CTA-Derived Products:				
living	cum-M _x -dit	15	C ₁₀₄ H ₁₈₀ N ₁₆ O ₁₅ S ₂ K ⁺	1996.28
disproportionation + transfer	cum-M _x -H	15	C ₁₀₅ H ₁₈₈ N ₁₆ O ₁₆ K ⁺	1968.39
disproportionation	cum-M _x -doub	15	C ₁₀₅ H ₁₈₆ N ₁₆ O ₁₆ K ⁺	1966.38
combination	cum-M _x -cum	15	C ₁₀₈ H ₁₈₇ N ₁₅ O ₁₅ K ⁺	1973.39
(ii) Initiator-Derived Products				
living	In-M _x -dit	15	C ₉₉ H ₁₇₅ N ₁₇ O ₁₅ S ₂ K ⁺	1945.26
disproportionation + transfer	In-M _x -H	15	C ₁₀₀ H ₁₈₃ N ₁₇ O ₁₆ K ⁺	1917.37
disproportionation	In-M _x -doub	15	C ₁₀₀ H ₁₈₁ N ₁₇ O ₁₆ K ⁺	1915.35
combination	In-M _x -in	16	C ₁₀₄ H ₁₈₈ N ₁₈ O ₁₆ K ⁺	1984.40
(iii) Mixed Combination Products				
combination	In-M _x -cum	16	C ₁₀₄ H ₁₈₈ N ₁₈ O ₁₆ K ⁺	1922.36

Scheme 3. Tentative Explanation of the Induction Period



which show a practically linear dependence on the RAFT agent concentration. Thus, induction and retardation seem to be correlated.

The reasons for the induction periods or retardation observed with some chain transfer agents are not clearly understood, but a number of possible explanations have been suggested:⁵ (a) slow fragmentation of the adduct formed from the initial RAFT agent; (b) slow fragmentation of the adduct formed from the polymeric RAFT agent; (c) slow reinitiation by the expelled radical; (d) tendency of the expelled radical to add to the RAFT agent rather than to monomer; (e) tendency of the propagating radical to add to the RAFT agent rather than to monomer.

Monteiro et al.¹³ suggested termination by addition of a propagating polymer chain to the adduct formed from the polymeric RAFT agent as a reason for retardation.

Barner-Kowollik et al.⁶ have reported an induction period for the RAFT polymerization of styrene with cumyl dithiobenzoate as chain transfer agent. They tentatively explained this observation by the formation of dicumyl radicals, Ph-C(S-cumyl)₂. This type of radicals has recently been observed experimentally using ESR spectroscopy.¹⁴ In our case, the induction periods might also be ascribed to the formation of dibenzyl or dicumyl RAFT radicals (**3** and **4**), respectively, via the reaction of excess benzyl CTA (**1**) with benzyl radicals or excess cumyl CTA (**2**) with cumyl radicals (Scheme 3).

This reaction will reduce the extent of reinitiation occurring until equilibrium is reached, resulting in an induction period. The observed induction periods agree well with simulations of Barner-Kowollik et al.⁶ The

longer induction period with the cumyl CTA would imply a higher stability of the dicumyl radicals as compared to the dibenzyl radicals. However, dicumyl radicals are expected to fragment more easily than dibenzyl radicals. Therefore, another explanation has to be envisaged. In a recent paper by Donovan et al.,¹⁵ similar induction periods are observed in the polymerization of *N,N*-dimethylacrylamide with cumyl and benzyl dithiobenzoate, respectively. As in the present work, the cumyl CTA shows a longer induction period as compared to the benzyl CTA of the same concentration. The authors ascribed this result to the different stabilities of the cumyl and benzyl radicals. Considering the radical stability, the bulky cumyl radical adds slower to NIPAAm monomer than the primary benzyl radical. Thus, the benzyl radical is expected to be a better initiating species.

UV and MALDI-TOF MS Analysis of the Polymers. The formation of the dithiocarbamate end groups of the resultant polymers is proven by both UV and MALDI-TOF spectroscopy. The UV spectrum shows a perceptible band with a maximum at $\lambda = 296$ nm in chloroform, which is ascribed to the pyrrolicarbothioate moiety.

MALDI-TOF mass spectra of the obtained RAFT polymers can indicate to which degree the polymerization is living and give information on the nature of the end groups. In RAFT polymerizations using cumyl (cum) dithiocarbamate (dit) as CTA, the products given in Table 2 can be expected in principle (see Figure 5b for structures).

In the literature, only two references on the MALDI-TOF characterization of RAFT polymers exist. Destarac et al.¹⁶ report the MALDI-TOF mass spectrum of poly(vinyl acetate) obtained by RAFT polymerization in bulk using AIBN as initiator and *S*-malonyl *N,N*-diphenyl-dithiocarbamate as chain transfer agent. They observed initiator-derived and hydrogen-terminated polymers. The formation of the latter was ascribed to transfer reactions since no olefinic end groups were found. Ganachaud et al.⁹ discuss the MALDI-TOF spectrum of poly(NIPAAm) obtained by RAFT polymerization in benzene with AIBN as initiator and benzyl dithiobenzoate as chain transfer agent. They report products resulting from termination by either disproportionation or transfer to monomer. However, they found only olefinic end groups, but no hydrogen-terminated chains, as one would expect for the disproportionation or transfer products.

Figures 4 and 5 show the MALDI-TOF mass spectra of poly(NIPAAm) obtained with benzyl CTA and cumyl CTA, respectively.

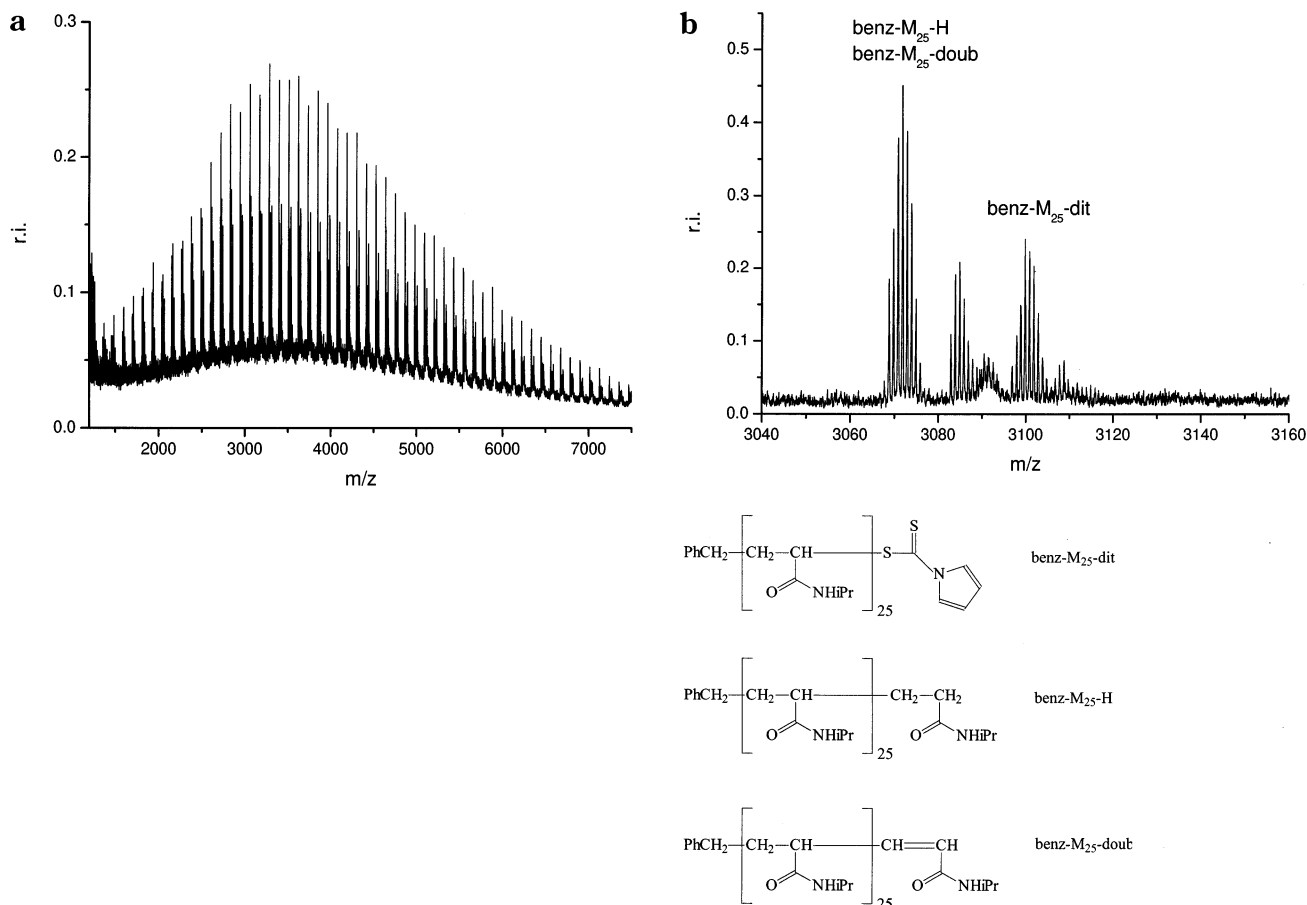


Figure 4. MALDI-TOF mass spectrum of poly(*N*IPAAm) with benzyl CTA (sample taken at 41% conversion). (a) Complete spectrum of K⁺-ionized sample. (b) Determination of the chain-end structures.

In both spectra, the expected signals (isotopic patterns) of the polymer with transfer agent end groups are observed (benz-M_x-dit and cum-M_x-dit, respectively). Besides these signals, signals ascribed to hydrogen- and double bond-terminated products (benz-M_x-doub/benz-M_x-H and cum-M_x-doub/cum-M_x-H, respectively) for both samples are found. On first sight, these might be ascribed to products of disproportionation and transfer (see below). In the case of the cumyl chain transfer agent (Figure 5b), initiator-derived polymers (in-M_x-dit, in-M_x-doub, in-M_x-H, in-M_x-in) were observed due to a very good signal-to-noise ratio and due to the low monomer conversion (13%) of the sample. The intensity of the corresponding initiator-derived polymer signals is very low so that a good resolution is necessary, which might explain why these products have not been detected before.⁹

In the MALDI-TOF spectra of the two different polymer samples, there are peaks that cannot be ascribed to the expected chain-end structures. The K⁺-ionized MALDI spectrum of the polymer obtained with cumyl CTA, for example (Figure 5b), reveals two series of signals with good isotopic resolution (1980.10, 2003.97 g/mol) and another rather noisy signal (1987–1990 g/mol) that cannot be ascribed to any of the possible structures expected from the synthesis. One of the signals (1980.10 g/mol) fits the CTA-derived main product (cum-M_x-dit) as Na⁺ adduct. However, closer inspection of the Na⁺-ionized MALDI spectra shows the same series of signals as in the K⁺-ionized samples shifted by the Na⁺ to K⁺ mass difference of 16 g/mol. This seems to identify this signal as a K⁺ adduct of a

chain with unknown end group structure. The signal at about 1987 g/mol is probably the result of a fragmentation in the flight tube. If the other two signals are also the result of a fragmentation under MALDI conditions, they must have formed in the ion source during ionization rather than during the flight time because of their good resolution. The occurrence of fragmentation during ionization in the MALDI-TOF analysis of dithiocarbamate-terminated polymers has already been reported by Beyou et al.¹⁷ They prepared dithiocarbamate-terminated polystyrene via the substitution of nitroxide moieties by dithiocarbamate moieties in polystyrene obtained by nitroxide-mediated free radical polymerization.

The MALDI-TOF spectra show that the peaks ascribed to disproportionation/transfer products have the highest intensity of all signals. This is a quite unexpected result as a combination of growing radicals is expected for poly(*N*-isopropylacrylamide) rather than disproportionation. Moreover, kinetics indicate only little termination and transfer. This becomes evident from the linear first-order time-conversion plot, especially at low monomer conversion (Figure 3), and from the plot of *M_n* vs conversion (Figures 8 and 9). Therefore, the question arises whether these signals are due to fragmentation of the polymer during the MALDI-TOF measurement. Furthermore, the relative intensities of double-bond terminated structures (cum-M_x-doub) to hydrogen terminated ones (cum-M_x-H) is not 1:1 but 1:(2.5 ± 1), which was confirmed by a simulation of the corresponding overlapping isotopic patterns (Figure 5c).

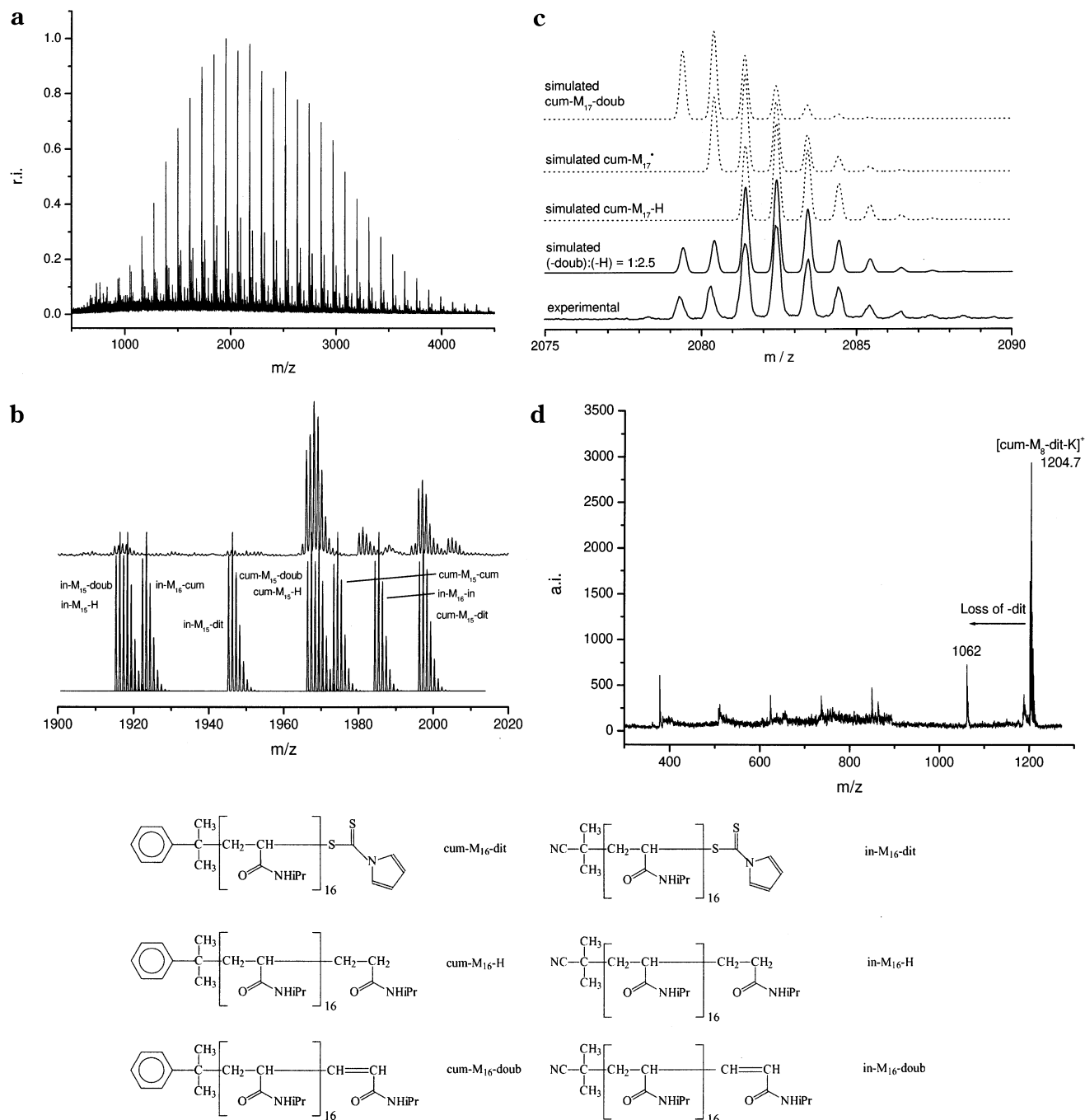


Figure 5. MALDI-TOF mass spectrum of poly(NIPAAm) with cumyl CTA (sample taken at 13% conversion). (a) Complete spectrum of K^+ -ionized sample. (b) Determination of the chain-end structures, with experimental (top) and simulated (bottom) data. (c) Simulation of signal overlap of assumed disproportionation/transfer signals. (d) Post source decay MALDI-TOF mass spectrum of poly(NIPAAm) with the composition cum- M_8 -dit. The most intense fragment peak corresponds to the loss of the dit residue.

The higher amount of cum- M_x -H chains might result from the cum- M_x radicals abstracting protons from the matrix during desorption. One possibility to prove this assumption is to perform a fragmentation analysis of the CTA-derived polymeric chains cum- M_x -dit- K^+ in the MALDI experiment. For this purpose, a post source decay (PSD) analysis¹⁸ was performed which showed that cum- M_x -dit- K^+ ions readily fragment under loss of the dit end group and formation of the corresponding cum- M_x -doub or cum- M_x -H chains but also into other fragments (Figure 5d), which corroborates the aforementioned conclusions. This result does not exclude the formation of cum- M_x -doub by the synthetic process but strongly indicates that the corresponding peaks stem

from fragmentation during ionization. Another indication of the fragmentation occurring during ionization is found in the MALDI-TOF spectrum of the hydrolyzed polymer. The spectrum shows no hydrogen- and double bond-terminated structures. This proves that these end groups do not result from the polymerization procedure but from fragmentation of the dithio moiety during ionization. Since λ_{\max} of the dithioester moiety (296 nm) is also close to the laser frequency (337 nm) for the MALDI process, this observation is not surprising. Our findings suggest that the signals attributed to disproportionation/transfer by other authors^{9,16} may also result from fragmentation.

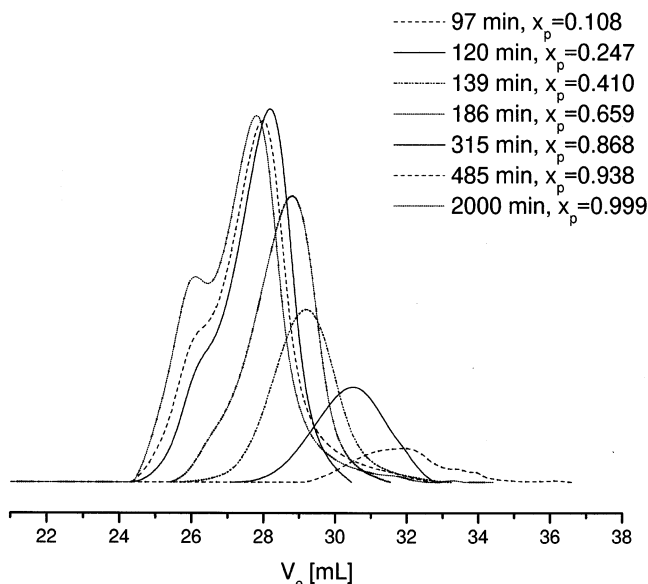


Figure 6. GPC traces (RI detector) of poly(NIPAAm) at different monomer conversions x_p in THF with 0.25% TBAB for the polymerization with a benzyl CTA concentration of 19.6 mmol/L.

GPC Analysis of the Polymers. The GPC characterization of poly(*N*-isopropylacrylamide) in THF involves various problems^{19,20} due to irreversible chain aggregation after complete drying of the polymer samples.⁹ Nevertheless, we have obtained good results by the addition of 0.25 wt % tetrabutylammonium bromide (TBAB) to the THF solution and using PSS SDVgel columns, whereas with pure THF no analysable results could be obtained.

Figures 6 and 7 show the GPC traces of poly(NIPAAm) at different monomer conversions for the polymerization with benzyl CTA and cumyl CTA, respectively.

For conversions higher than 90%, a high-molecular weight shoulder is observed. This is usually observed for RAFT polymers⁹ at high monomer conversions, which is most likely due to combination of the growing chains.

Figures 8 and 9 show the dependences of M_n (determined by MALDI-TOF MS) and PDI on conversion for benzyl CTA and for cumyl CTA, respectively, as chain transfer agent.

The straight lines in Figure 8 represent the dependence of the calculated number-average molecular weight on conversion,

$$M_{n,theor} = \frac{[M]_0}{[CTA]_0} x_p M_{monomer} + M_{CTA}$$

where x_p denotes monomer conversion and $[M]_0$ and $[CTA]_0$ are the initial concentrations of monomer and chain transfer agent, respectively. The linearity of the plots indicates the absence of irreversible transfer reactions. The slight increase at high conversions is ascribed to combination reactions of the living polymer chains.

The agreement of the experimental M_n values with the calculated ones is better for benzyl CTA as chain transfer agent than for cumyl CTA (see Table 1). This may be explained by the higher impurity (approximately 5%, as determined by ¹H NMR spectroscopy) of the cumyl RAFT agent. The polydispersity indices decrease with increasing conversion (Figure 9) except at high conversion, due to combination of growing chains at high conversion, which is typical for controlled polymerizations with exchange between active and dormant species.²¹

GPC evaluation of the molecular weights using polystyrene standards for calibration gives significantly higher molecular weights than those obtained from MALDI-TOF analysis (Figure 10). The difference be-

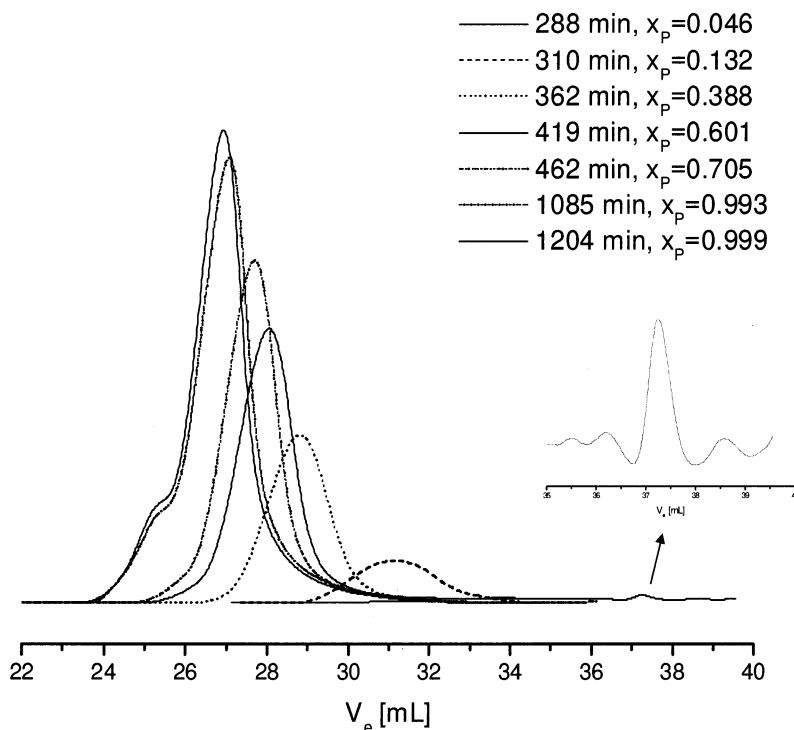


Figure 7. GPC traces (RI detector) of poly(NIPAAm) at different monomer conversions x_p in THF with 0.25% TBAB for the polymerization with cumyl CTA.

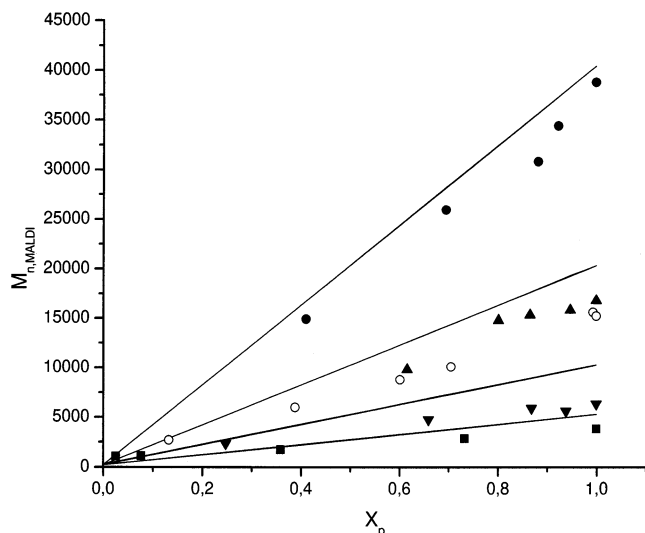


Figure 8. Dependence of $M_n(\text{MALDI})$ on monomer conversion for benzyl and cumyl CTA. Key: (■) benzyl CTA with $[\text{CTA}]_0 = 3.92 \times 10^{-2}$, (▼) 1.96×10^{-2} , (▲) 9.80×10^{-3} , (●) and 4.90×10^{-3} mol/L; (○) cumyl CTA with $[\text{CTA}]_0 = 1.96 \times 10^{-2}$ mol/L; (---) $M_n(\text{theor})$.

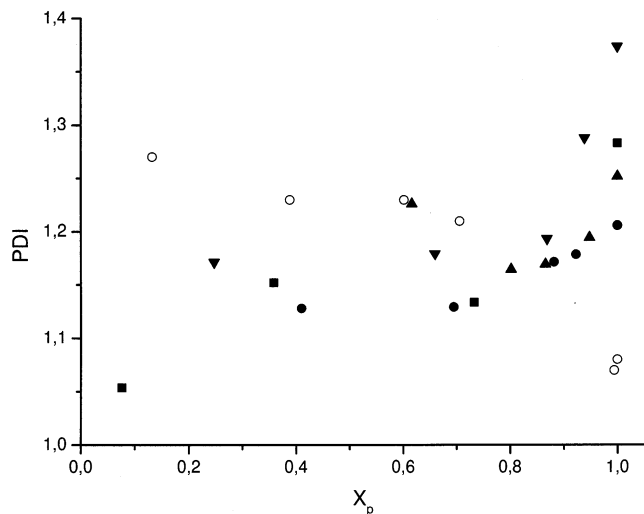


Figure 9. Dependence of PDI (from GPC with PNIPAAm calibration) on conversion for benzyl and cumyl CTA. For symbols, see Figure 8.

tween $M_n(\text{MALDI})$ and $M_n(\text{GPC})$ is much more pronounced than the one reported for poly(NIPAAm) by Ganachaud et al.⁹ who used THF GPC to determine the molecular weights. The maximum deviation with a ratio of $M_n(\text{GPC})/M_n(\text{MALDI}) \approx 4$ is observed at $M_n(\text{GPC}) \approx 25\,000$ g/mol. A linear fit of the bilogarithmic plot of $M_n(\text{MALDI})$ vs $M_n(\text{GPC})$ for the poly(NIPAAm) samples obtained with benzyl CTA (Figure 10) results in the relation

$$\log M_n(\text{MALDI}) = -3.23(\pm 0.32) + 1.577(\pm 0.069) \log M_n(\text{GPC})$$

The linear relationship between $\log M_n(\text{MALDI})$ and $\log M_n(\text{GPC})$ is based on the linearity of the Mark–Houwink relation which typically holds true for $M_n \geq 10^4$ g/mol. The fit was therefore only applied to $\log M_n(\text{MALDI}) > 3.8$; corresponding to $M_n(\text{GPC}) > 4.4$. If all values are considered, a second-order polynomial

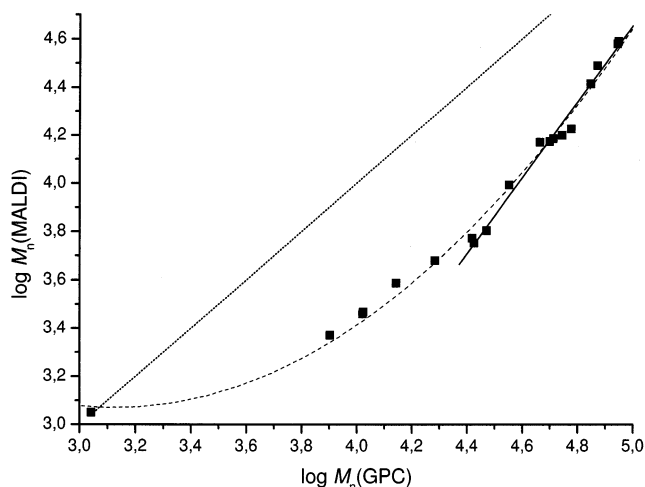


Figure 10. Bilogarithmic plot of $M_n(\text{MALDI})$ vs $M_n(\text{GPC})$ for the polymerization with benzyl CTA: (—) linear fit of data points for $\log M_n(\text{MALDI}) > 3.8$; (---) second-order polynomial fit of all data points; (···) line expected for $M_n(\text{MALDI}) = M_n(\text{GPC})$.

approximates the values:

$$\log M_n(\text{MALDI}) = 7.44 - 2.80 \log M_n(\text{GPC}) + 0.448 [\log M_n(\text{GPC})]^2$$

For the polymerization with cumyl CTA, slightly higher $M_n(\text{MALDI})$ values are obtained as compared to the polymerization with benzyl CTA. Most of these samples had molecular weights $M_n(\text{GPC})$ below 25 000 so that they were not considered in the linear fit.

Conclusions

The RAFT polymerization of *N*-isopropylacrylamide with two different chain transfer agents, namely benzyl 1-pyrrolicarbodithioate and cumyl 1-pyrrolicarbodithioate, results in polymers with narrow MWDs as well as M_n values that are in good agreement with the calculated ones. A comparison between the M_n values determined from GPC and the values from MALDI–TOF MS shows that the molecular weights obtained from GPC using polystyrene standards are much too high.

In situ FT-NIR spectroscopy is a powerful technique for the reliable determination of monomer conversions in the RAFT polymerization of *N*-isopropylacrylamide. In our case, it became evident that both polymerization processes show an induction period that seems to be correlated with a retardation in rate, where the induction time is higher for the cumyl CTA as compared to the benzyl CTA of the same concentration. The induction periods might be explained in terms of the different stabilities of the respective radicals that add to monomer in the reinitiation step. The more stable cumyl radical adds slower than the benzyl radical.

The MALDI–TOF characterization of the polymer samples showed that the produced polymers possess the expected transfer agent end groups together with some initiator-derived polymers. End groups that seemed to originate from disproportionation or transfer are likely the result of fragmentation under MALDI conditions.

Acknowledgment. The authors wish to thank Dr. Ezio Rizzardo and Dr. San Thang, CSIRO Molecular Science, for fruitful discussions and helpful hints and

Cornelia Lauble for her help with the MALDI-TOF measurements. We also would like to thank the reviewers for their constructive comments.

References and Notes

- (1) Chong, Y. K.; Le, T. P. T.; Moad, G.; Rizzardo, E.; Thang, S. H. *Macromolecules* **1999**, *32*, 2071–2074.
- (2) Mayadunne, R. T. A.; Rizzardo, E.; Chiefari, J.; Chong, Y. K.; Moad, G.; Thang, S. H. *Macromolecules* **1999**, *32*, 6977–6980.
- (3) Rizzardo, E.; Chiefari, J.; Mayadunne, R. T. A. In *Controlled/Living Radical Polymerization—Progress in ATRP, NMP, and RAFT*; Matyjaszewski, K., Ed.; ACS Symposium Series 768; American Chemical Society: Washington, DC, 2000; Vol. 768, pp 278–295.
- (4) Chiefari, J.; Chong, Y. K.; Ercole, F.; Krstina, J.; Jeffery, J.; Le, T. P. T.; Mayadunne, R. T. A.; Meijs, G. F.; Moad, C. L.; Moad, G.; Rizzardo, E.; Thang, S. H. *Macromolecules* **1998**, *31*, 5559–5562.
- (5) Moad, G.; Chiefari, J.; Chong, Y. K.; Krstina, J.; Mayadunne, R. T. A.; Postma, A.; Rizzardo, E.; Thang, S. H. *Polym. Int.* **2000**, *49*, 993–1001.
- (6) Barner-Kowollik, C.; Quinn, J. F.; Morsley, D. R.; Davis, T. P. *J. Polym. Sci., Part A: Polym. Chem.* **2001**, *39*, 1353–1365.
- (7) Goto, A.; Sato, K.; Tsujii, Y.; Fukuda, T.; Moad, G.; Rizzardo, E.; Thang, S. H. *Macromolecules* **2001**, *34*, 402–408.
- (8) Long, T. E.; Liu, H. Y.; Schell, B. A.; Teegarden, D. M.; Uerz, D. S. *Macromolecules* **1993**, *26*, 6237–6242.
- (9) Ganachaud, F.; Monteiro, M. J.; Gilbert, R. G.; Dourges, M.-A.; Thang, S. H.; Rizzardo, E. *Macromolecules* **2000**, *33*, 6738–6745.
- (10) Chiefari, J.; Mayadunne, R. T. A.; Moad, G.; Rizzardo, E.; Thang, S. H. WO 99/31144 (inventors: DuPont Co.), 1999.
- (11) Schilli, C.; Müller, A. H. E. *SML'01 International Symposium on Free Radical Polymerization: Kinetics and Mechanism, Il Ciocco, Italy*, 2001.
- (12) Lanzendörfer, M.; Schmalz, H.; Abetz, V.; Müller, A. H. E. *Polym. Prepr. (Am. Chem. Soc., Div. Polym. Chem.)* **2001**, *42*, 329–330.
- (13) Monteiro, M. J.; Brouwer, H. d. *Macromolecules* **2001**, *34*, 349–352.
- (14) Calitz, F. M.; Tonge, M. P.; Sanderson, R. D. *5th Annual UNESCO School and Conference on Macromolecules & Materials Science, Stellenbosch, South Africa*, 2002.
- (15) Donovan, M. S.; Lowe, A. B.; Sumerlin, B. S.; McCormick, C. L. *Macromolecules* **2002**, *35*, 4123–4132.
- (16) Destarac, M.; Charmot, D.; Franck, X.; Zard, S. Z. *Macromol. Rapid Commun.* **2000**, *21*, 1035–1039.
- (17) Beyou, E.; Chaumont, P.; Chauvin, F.; Devaux, C.; Zydowicz, N. *Macromolecules* **1998**, *31*, 6828–6835.
- (18) Kaufmann, R.; Spengler, B.; Lutzenkirchen, F. *Rapid Commun. Mass Spectrom.* **1993**, *7*, 902–910.
- (19) Cole, C.-A.; Schreiner, S. M.; Monji, N. *Polym. Prepr. (Am. Chem. Soc., Div. Polym. Chem.)* **1986**, *27* (1), 237–238.
- (20) Yang, H. J.; Cole, C.-A.; Monji, N.; Hoffman, A. S. *J. Polym. Sci., Part A: Polym. Chem.* **1990**, *28*, 219–226.
- (21) Litvinenko, G. I.; Simon, P. F. W.; Mueller, A. H. E. *Macromolecules* **1999**, *32*, 2410–2419.

MA0121159